Supporting Information

Catalytic Performance of Mixed $M_xCo_{3-x}O_4$ (M = Cr, Fe, Mn, Ni, Cu, Zn) Spinels Obtained by Combustion Synthesis for Preferential Carbon Monoxide Oxidation (CO-PROX) – Insights into the Factors Controlling the Catalysts Selectivity and Activity

Camillo Hudy[1], Olga Długosz[2], Joanna Gryboś[1], Filip Zasada[1], Aneta Krasowska[1], Janusz Janas[1], Zbigniew Sojka[1]

*Corresponding Authors: C. Hudy, Z. Sojka

A) Table S1. Average crystallite size and strains calculated by Williamson-Hall method along with the BET surface area.

Sample	Williamson-Hall method *d* / nm	Strain /10^{-3}	Surface area / $m^2\,g^{-1}$
Cr-Co	27.4	19.6	15.1
Mn-Co	20.5	12.4	16.8
Fe-Co	20.8	7.3	15.9
Co_3O_4	49.6	2.7	10.0
Ni-Co	46.6	5.4	11.7
Cu-Co	52.1	3.8	8.9
Zn-Co	52.7	7.4	14.9

B) Sample imaging by Scanning Electron Microscopy

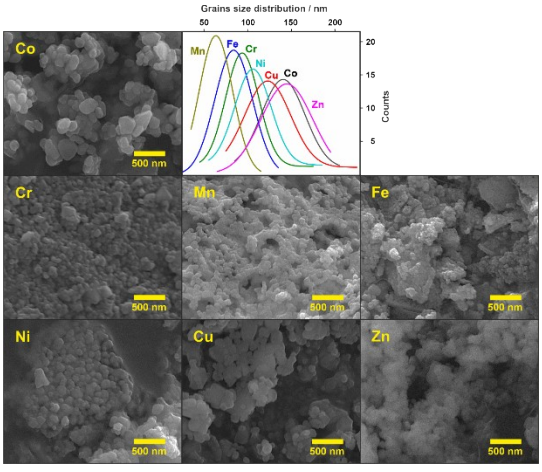

Figure S1. The SEM images along with the fitted Gauss curves based on the grains size distribution.

C) XPS spectra of the catalysts

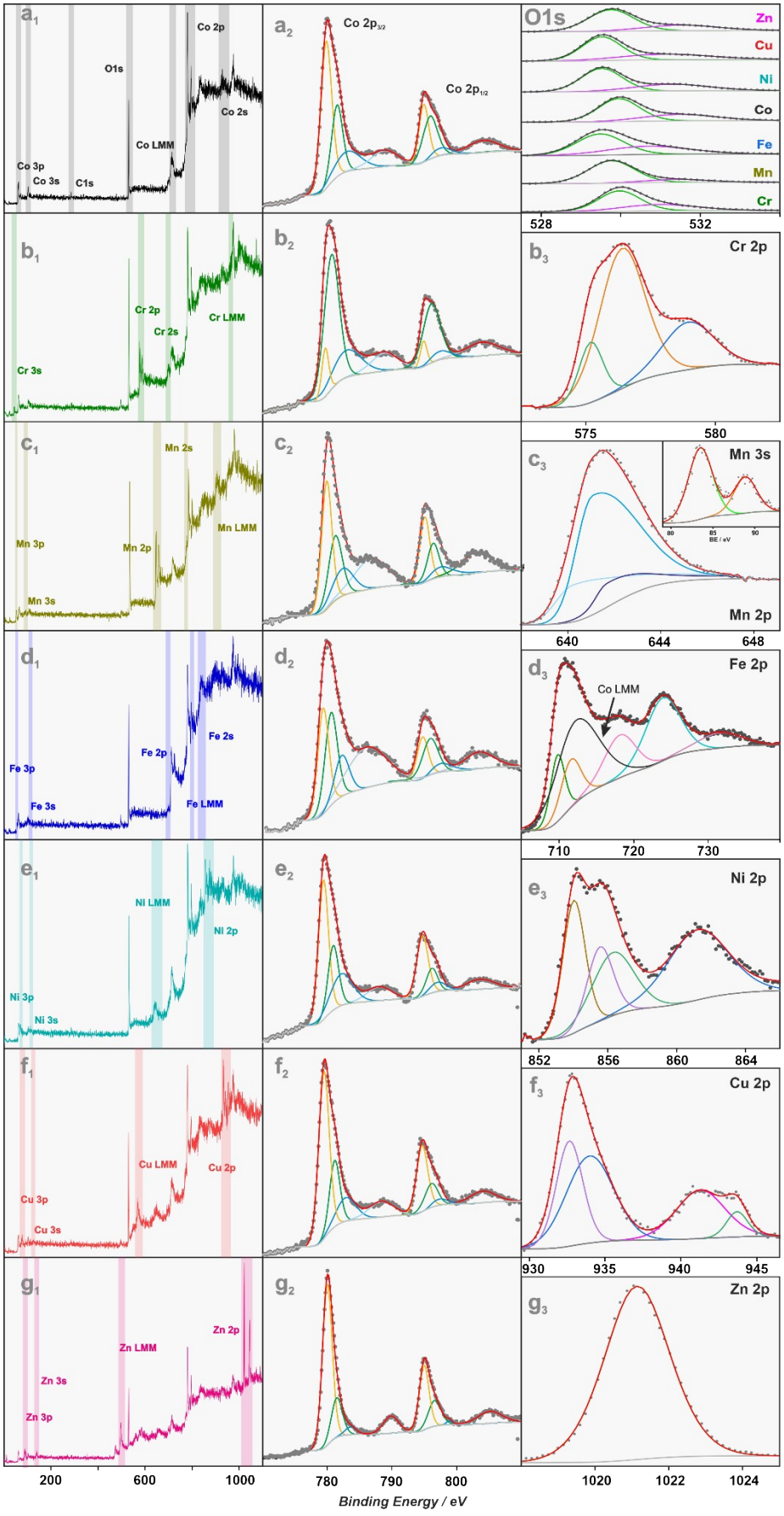

Figure S2. The deconvoluted XPS spectra: a_1 – g_1 show full range spectra in following order Co(a). Cr-Co(b). Mn-Co(c). Fe-Co(d). Ni-Co(e). Cu-Co(f). Zn-Cu(g). a_2 – g_2 show Co_{2p} range and b_3 – g_3 2p range of proper heterometal. The right-upper corner shows the spectra of the O1s range of each sample.

Table S2. Chemical composition of the samples determined by XRF and XPS techniques along with the calculated formulas along with the calculated Co^{3+}/Co^{2+} ratio.

Sample	M/Co		Chemical Formula	
	XRF	XPS	bulk	surface
Cr-Co	0.49	0.54	$Cr_{0.98}Co_{2.02}O_4$	$Cr_{1.08}Co_{1.98}O_4$
Mn-Co	0.51	0.65	$Mn_{1.02}Co_{1.98}O_4$	$Mn_{1.3}Co_{1.7}O_4$
Fe-Co	0.42	0.67	$Fe_{0.84}Co_{2.16}O_4$	$Fe_{1.34}Co_{1.66}O_4$
Co	-		Co_3O_4	
Ni-Co	0.65	0.84	$Ni_{1.3}Co_{1.7}O_4$	$Ni_{1.68}Co_{1.32}O_4$
Cu-Co	0.46	0.48	$Cu_{0.92}Co_{2.08}O_4$	$Cu_{0.96}Co_{2.08}O_4$
Zn-Co	0.46	0.62	$Zn_{0.92}Co_{2.08}O_4$	$Zn_{1.24}Co_{1.76}O_4$

D) The Rietveld refinement of the XRD patterns

The results of Rietveld refinement were obtained for the series of synthesized materials. Chemical composition revealed by XPS measurements was applied as the initial information for phase composition optimization. The quality of the Rietveld fit was checked by the reliability coefficients *R*, which should be less than 10%. and by the fit coefficient χ^2, which should be close to one[1]. The final Rietveld fit resulted in R_P of 0.6-1.19, R_B ranging from 7.3-21.8, R_F ranging from 6.78 to 15.7, and χ^2 ranging from 1.3 to 2.7. Similar high values of *R*-factors for nanocrystalline materials were observed by other authors[2,3]. The reason may be due to the relatively large background noise in the XRD patterns of nanocrystalline materials, which was noticed especially for Fe-Co, Cu-Co, and Mn-Co. Meanwhile low χ^2 values were observed justifying the fit. The increased R_B values were related to the size of the nanocrystals. In the diffraction patterns, diffusive scattering becomes significant due to the large ratio of surface atoms to volume atoms. At the same time the Bragg scattering is reduced, due to decrease in the crystallinity, leading to large *R* factors[4].

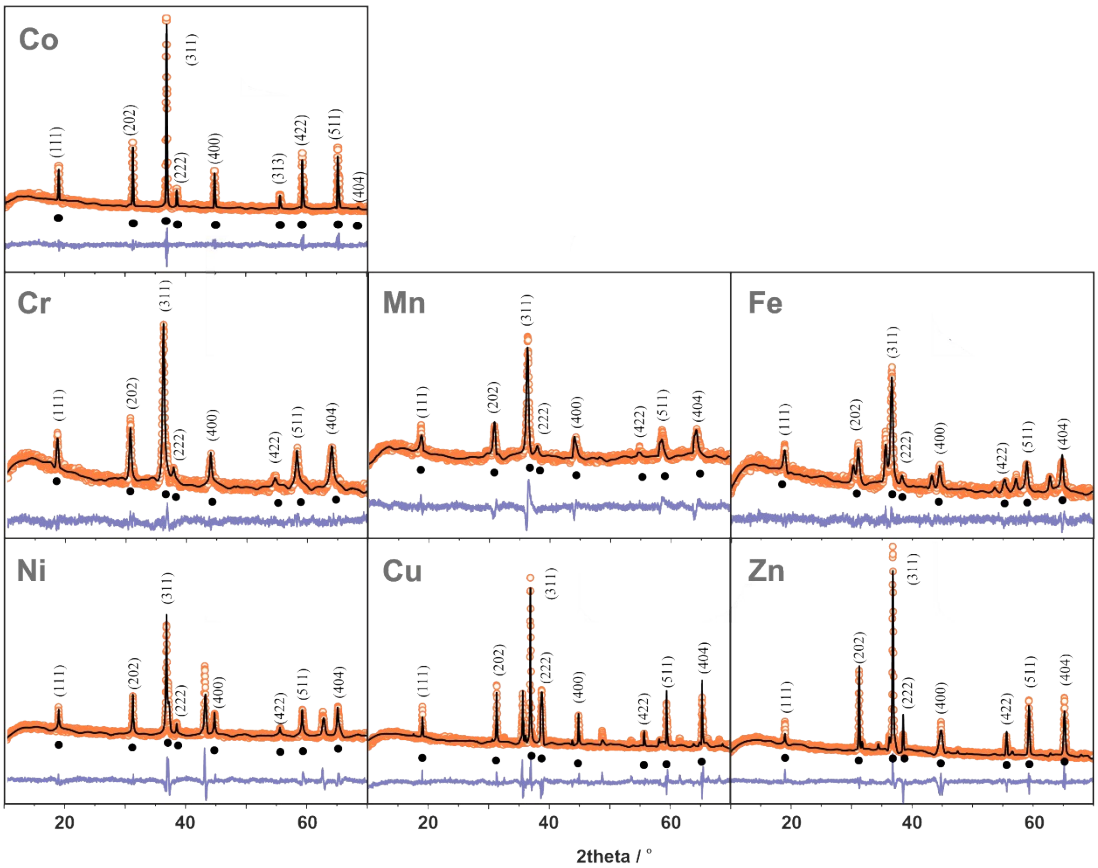

Figure S3. The experimentally obtained XRD patterns (orange dots) along with the fitted Rietveld model (black line) and disparity of data (purple line below). Marked peak positions corresponds to the $(M_xCo_{1-x})[Co_{2-y}M_y]O_4$ phase.

Table S3. Rietveld refinement parameters, lattice parameter and volume of the unit cell of Co and M-Co spinels.

Catalysts	R_P [%]	R_B [%]	R_F [%]	χ^2	V [Å]
Cr-Co	1.06	10.2	15.4	1.8	578.97
Mn-Co	1.08	16.8	13.3	1.6	562.39
Fe-Co	0.76	21.8	11.7	1.3	540.07
Co_3O_4	0.60	7.3	8.4	1.8	528.92
Ni-Co	1.19	8.1	6.9	2.7	530.69
Cu-Co	0.61	14.5	15.2	2.7	529.22
Zn-Co	0.78	12.0	10.4	1.7	530.81

R_P – profile factor. R_B – Bragg factor. R_F – crystallographic factor. χ^2 – goodness of fit factor. V – unit cell volume

E) The temperature-programmed H_2 reduction

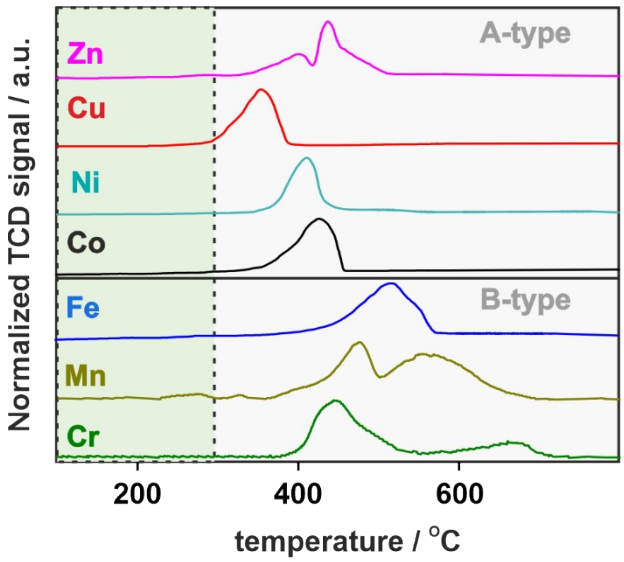

Figure S4. Temperature-programmed H_2-reduction Green area corresponds to the PROX temperature window.

F) Parity plots for CO and H_2 oxidation alone and in the CO-PROX reaction

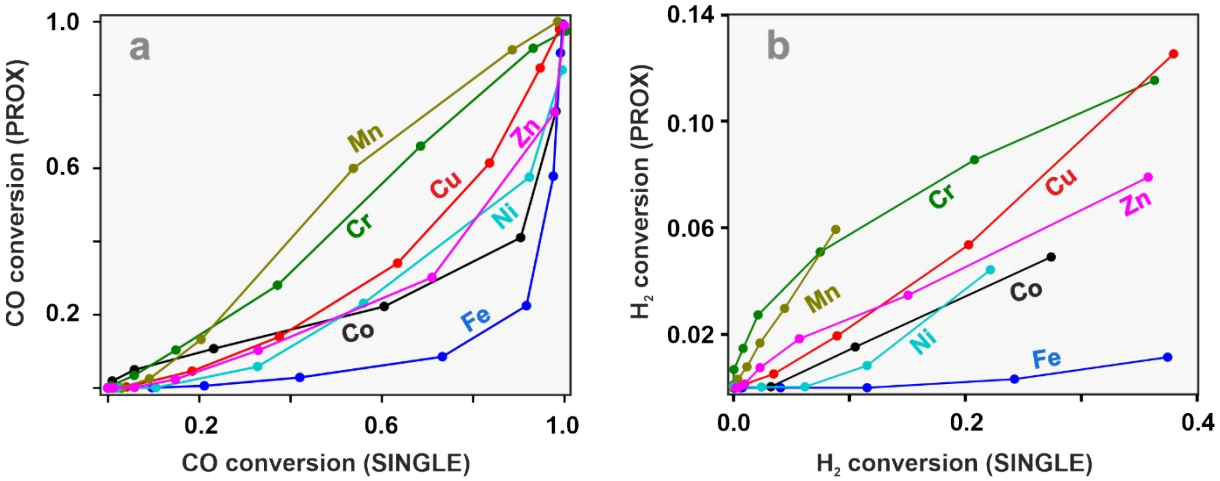

Fig. S5. Parity plots sole CO oxidation vs CO oxidation in PROX conditions (a) sole H_2 oxidation vs H_2 oxidation in PROX conditions (b).

G) Reproducibility of PROX reaction

To evaluate the catalytic stability four consecutive PROX runs (with after going cooling in the inert gas flow) on the reference Co_3O_4 spinel were conducted. and the results are show on the **Figure S6.**

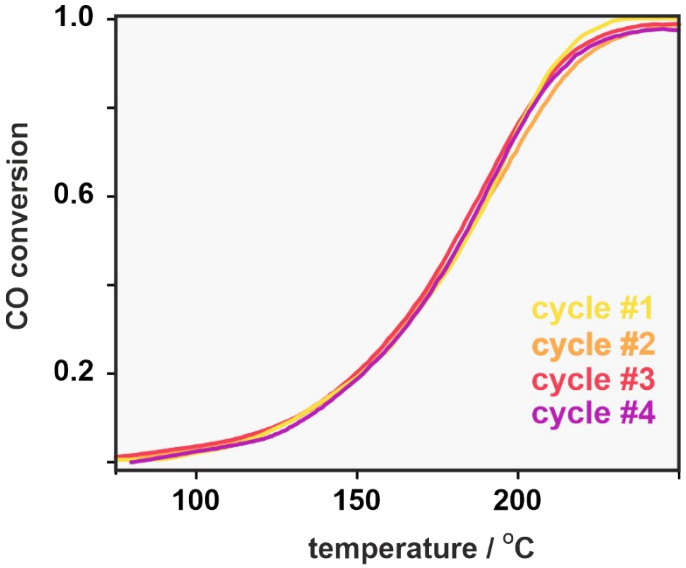

Figure S6. The reproducibility of CO conversion over Co_3O_4 measured within four consecutive cycles of PROX process.

H) Assessment of the CO methanation

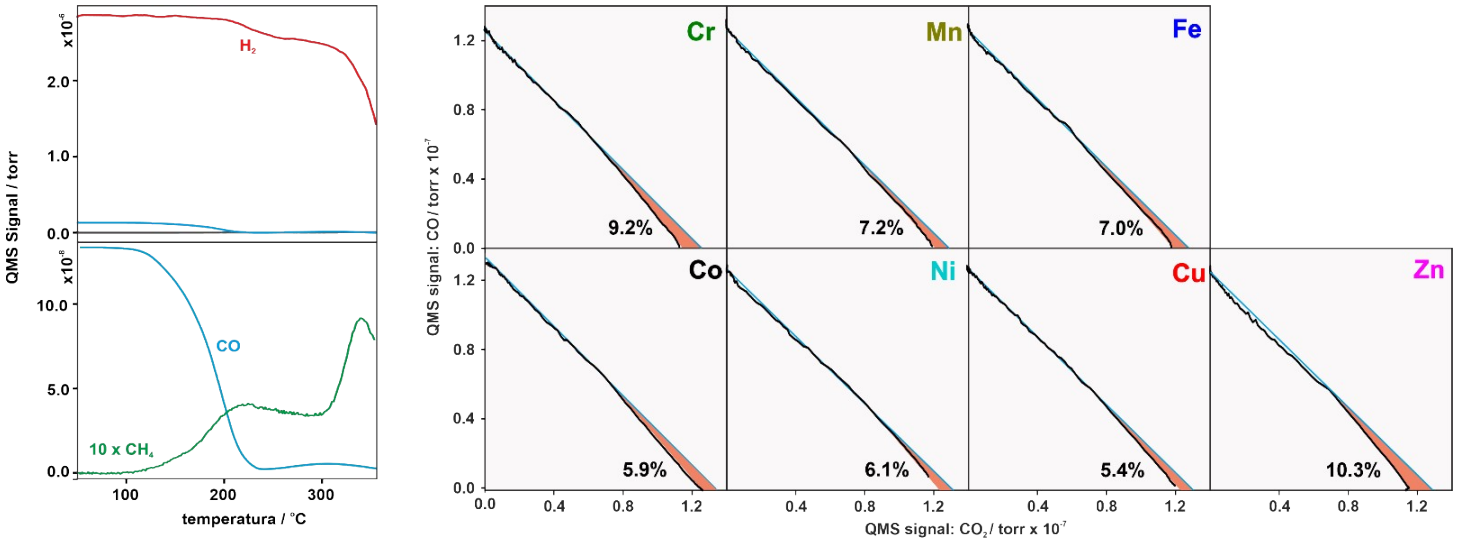

Figure S7. Formation of CH_4 during the CO-PROX reaction over Co_3O_4 catalyst. QMS profiles of (left) and the CO vs CO_2 parity (right) showing the divergence in the high temperature region associated with the CH_4 formation.

I) Metal 3d and oxygen 2p band centers and Pauling electronegativities

Table S4. The positions of the metal and oxygen band centers, calculated by Sun et. al[5] along with the Pauling electronegativities.

Mixed spinel formula	Oxygen 2p band center E_{O2p}/eV	Metal 3d band center (max $\{M_{A\text{-}3d}, M_{B\text{-}3d}\}$) E_{Md3}/eV	Pauling electronegativity
$Co[Cr_{1.75}Co_{0.25}]O_4$	-2.503	-1.769	1.7
$[Mn_{0.125}Co_{0.875}][Mn_{0.875}Co_{1.125}]O_4$	-2.573	-1.292	1.6
$[Fe_{0.5}Co_{0.5}][Fe_{0.5}Co_{1.5}]O_4$	-3.416	-2.091	1.8
$CoCo_2O_4$	-2.336	-1.204	1.9
$[Ni_{0.5}Co_{0.5}][Ni_{0.5}Co_{1.5}]O_4$	-2.176	-1.538	1.9
$Co[Cu_{0.25}Co_{1.75}]O_4$	-1.525	-1.220	1.9
$[Zn_{0.875}Co_{0.125}]Co_2O_4$	-1.338	-0.638	1.7

Biography

1 D. Kaczorowski, E. Murashova, Z. Kurenbaeva and A. Gribanov, *J. Alloys Compd.*, 2019, **802**, 437–444.

2 B. Mandal, M. R. Das and P. Mitra, *J. Alloys Compd.*, 2019, **784**, 877–886.

3 G. R. Reddy, G. R. Dillip, T. V. M. Sreekanth, R. Rajavaram, B. D. P. Raju, P. C. Nagajyothi and J. Shim, *Appl. Surf. Sci.*, 2020, **529**, 147123.

4 A. Kumar, Undesrstanding Complex Orderding In Transition Metal Oxides, *Doctoral Thesis*, West Bengal University of Technology, 2013.

5 Y. Sun, H. Liao, J. Wang, B. Chen, S. Sun, S. J. H. Ong, S. Xi, C. Diao, Y. Du, J. O. Wang, M. B. H. Breese, S. Li, H. Zhang and Z. J. Xu, *Nat. Catal.*, 2020, **3**, 554–563.